

# EEGVid: Dynamic Vision from EEG Brain Recordings, How much does EEG know?

Prajwal Singh<sup>†</sup>   Anupam Sharma   Pankaj Pandey  
 Krishna Miyapuram   Shanmuganathan Raman<sup>†</sup>  
 CVIG Lab<sup>†</sup> and BraIn Lab  
 IIT Gandhinagar

{singh\_prajwal, sharmaanupam, pankaj.p, kprasad, shanmuga}@iitgn.ac.in

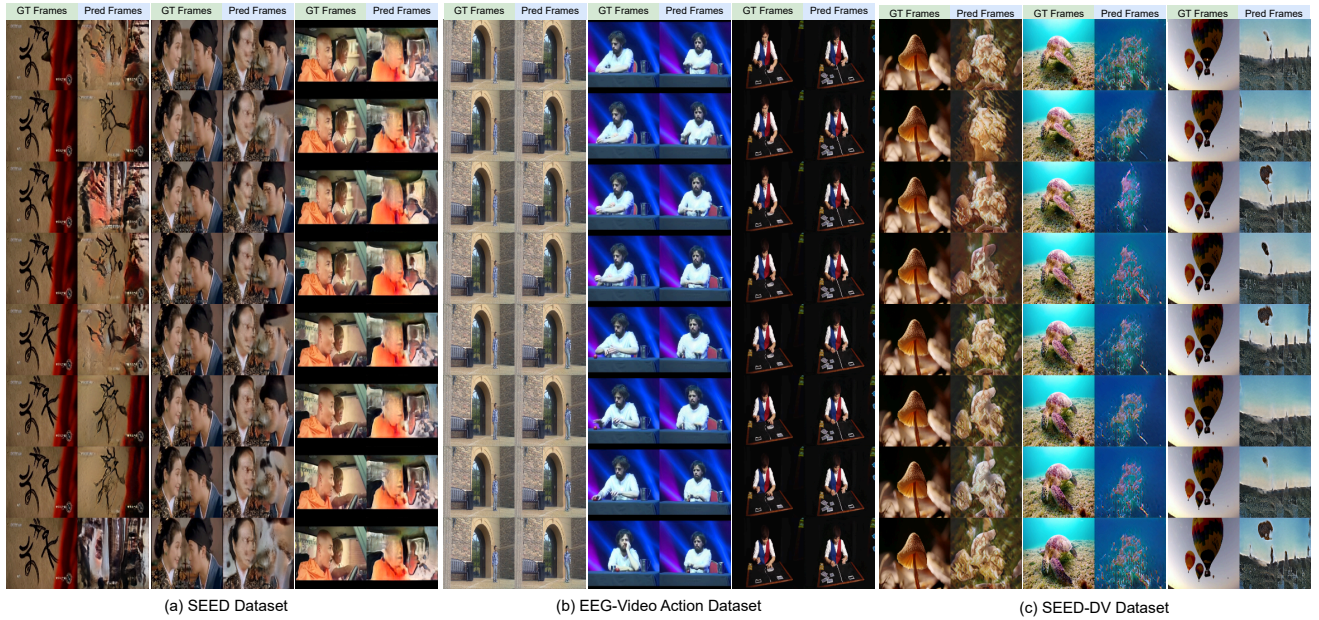


Figure 1. **Generated Video Frames from EEG.** Figure illustrates the synthesized video frames from EEG signals across diverse movie clips from the SEED [10, 64], EEG-Video Action [59], and SEED-DV [28] dataset that is shown to the participants. In our work, we have used eight frames per clip for synthesis results (8 fps).

## Abstract

*Reconstructing and understanding dynamic visual information (video) from brain EEG recordings is challenging due to the non-stationary nature of EEG signals, their low signal-to-noise ratio (SNR), and the limited availability of EEG-Video stimulus datasets. Most recent studies have focused on reconstructing static images from EEG recordings. In this work, we propose a framework to reconstruct dynamic visual stimuli from EEG data and conduct an in-depth study of the information encoded in EEG signals. Our approach first trains a feature extraction network using a triplet-based contrastive learning strategy within an EEG-video generation framework. The extracted EEG features are then used for video synthesis with a modi-*

*fied StyleGAN-ADA, which incorporates temporal information as conditioning. Additionally, we analyze how different brain regions contribute to processing dynamic visual stimuli. Through several empirical studies, we evaluate the effectiveness of our framework and investigate how much dynamic visual information can be inferred from EEG signals. The inferences we derive through our extensive studies would be of immense value to future research on extracting visual dynamics from EEG.*

## 1. Introduction

Decades of research have focused on understanding human perception, particularly the dynamic nature of visual

processing, where the brain interprets a continuous stream of diverse information. The question of how to comprehend this complexity has engaged cognitive scientists, neuroscientists, philosophers, and computer scientists alike [11, 15, 23, 54]. Recent advances in multi-modal representation learning and generative AI have enabled decoding neural activities, mainly using self-supervised and contrastive learning-based methods to align fMRI and EEG signals with pre-trained image or text modalities. However, it is crucial to investigate the inherent information contained within EEG signals without relying on alignment with other modalities.

To address this, we utilize emotion-based and non-emotion-based EEG-Video pairs to learn a dynamic visual EEG representation via contrastive learning with a triplet loss. This approach enforces the separation of dissimilar classes while bringing similar classes closer in representational space, facilitating the learning of discriminative features. Through this framework, we explore several key research questions (RQ), which are given below.

- **RQ1: How are emotional and visual features related?** Do visual features inherently encode emotional information, or are they distinct? Our findings indicate that visual representations retain emotional information, allowing emotion-based clustering.
- **RQ2: Do emotional or visual features retain subject-specific information?** EEG signals inherently exhibit subject-specific variations. Clustering representations from an untrained network naturally groups data by participants. However, learning visual or emotional representations diminishes this subject-specific information.
- **RQ3: How do different brain lobes contribute to processing visual and emotional features?** We observe that the temporal lobe plays a dominant role in encoding both emotional and visual representations. The frontal region contributes mainly to emotional features, whereas the posterior region, particularly the prenatal posterior region, is critical for visual representation.
- **RQ4: Can dynamic videos be faithfully reconstructed without alignment with other modalities?** We train a GAN-based model on extracted EEG features to explore this. Our quantitative results show that the generated frames align well with the videos shown to participants during EEG recording.

## 2. Related Work

### 2.1. Decoding Static Perception

Reconstructing visual images from brain activity has been widely studied using fMRI signals. Early work used linear or Bayesian models to map neural responses to visual stimuli [4, 31, 32, 40]. Miyawaki *et al.* [31] combined multi-scale decoders for basic pattern reconstruction, while Nas-

laris *et al.* [32] applied a Bayesian framework for natural images. Brouwer and Heeger [4] reconstructed color from early visual cortex responses, and Schoenmakers *et al.* [40] extended linear decoding techniques.

Recent approaches use deep learning for neural response mapping. Beliy *et al.* [1] and Gaziv *et al.* [13] applied self-supervised learning for natural image reconstruction. Lin *et al.* [26] proposed “Mind Reader” for complex image reconstruction. GAN-based methods [29, 35] improved semantic realism, building on earlier efforts [19, 36].

Latent diffusion models have recently emerged for high-resolution reconstruction. Takagi and Nishimoto [50], Chen *et al.* [7], and Sun *et al.* [48] conditioned diffusion pipelines on brain activity for detailed synthesis. Zeng *et al.* [62], Scotti *et al.* [43], and Xia *et al.* [58] introduced semantic and controllable conditioning to improve quality and interpretability. Ozelik and VanRullen [34] demonstrated latent diffusion for natural scene reconstruction, while shared-subject frameworks were explored in [2, 44]. Foundational work on diffusion models [16, 20, 39] supports these advances by enabling robust visual decoding from brain signals.

### 2.2. Decoding Dynamic Perception

Decoding dynamic perception from brain signals has advanced with models shifting from linear to diffusion-based frameworks. Videos are known to activate broader cortical regions than static images [5, 42, 60]. Several studies focus on reconstructing continuous video stimuli from fMRI [8, 12, 24, 49, 55, 57].

Wen *et al.* [57] used linear regression to estimate feature maps from fMRI, which were input to a Deconvolutional Neural Network [61]. Kupersmidt *et al.* [24] proposed an encoder-decoder model with a self-supervised stage that generated synthetic fMRI from video using a frozen encoder, then trained a decoder to reconstruct frames.

To improve data efficiency, Sun *et al.* [49] aligned fMRI features with CLIP [38] embeddings and used diffusion for video generation. Fosco *et al.* [12] followed a similar strategy with Masked Brain Modeling [7]. Chen *et al.* [8] added Spatiotemporal Attention to address spatial structure and hemodynamic lag [6]. GAN-based approaches have also been explored [55].

Despite progress, fMRI suffers from high cost and low temporal resolution. EEG offers a cheaper, high-temporal-resolution alternative. Liu *et al.* [28] introduced the SEED-DV dataset and a Seq2Seq model for reconstructing videos from EEG. However, the dataset has low class decoding accuracy, leading to poor EEG representations and unrealistic outputs. Unlike SEED-DV, our approach uses a GAN-based framework that synthesizes video directly from EEG features, avoiding cross-modal alignment [25] and reliance on large pre-trained networks.

### 3. Method

In this section, we will discuss how and why we have used a triplet loss-based feature extraction method [41] for learning EEG signal representation. Later, we will discuss how we can exploit the EEGStyleGAN-ADA [46] for EEG-based video-frame generation and its advantages over the diffusion-based method for video synthesis.

#### 3.1. Extracting Features from EEG

The most important step in generating videos from brain-recorded EEG signals is to extract meaningful visual features from them. We follow the established contrastive learning [30, 45] strategy for feature learning from EEG. We used a triplet-learning method [41] with an anchor ( $x^a$ ), positive ( $x^p$ ), and negative ( $x^n$ ) pair. As shown in Eqn. 1 triplet loss aims to keep the positive pair feature close to the anchor feature and contrast the negative pair feature. The  $\delta$  is the margin distance between the positive ( $x^p$ ) and negative ( $x^n$ ) anchor pair.

$$\min_{\theta} \mathbb{E} [\|f_{\theta}(x^a) - f_{\theta}(x^p)\|_2^2 - \|f_{\theta}(x^a) - f_{\theta}(x^n)\|_2^2 + \delta] \quad (1)$$

**Why use the Triplet Method?** In recent works [8, 12, 49] for representation learning from EEG signals, researchers are using contrastive language-image pre-training (CLIP) [38] where the feature of EEG is aligned with either pre-trained image or text modality features. Deviating from the recent strategy of learning representation using multi-modal learning, we use triplet loss for our work. It considers the labels to create positive and negative pairs and helps the network focus on distinct patterns in the EEG signals to learn the discriminative features. Such a fine-grained control is challenging to achieve using a CLIP-based multi-modal method. Furthermore, the recorded brain EEG signals, in our case, are responses to video-based stimuli; thus, the triplet loss-based method helps capture the meaningful feature that encodes video-based information.

Another important aspect of learning the representation from the EEG signal is the encoder architecture. In our work, we have used a modified NICE EEG [47] network. As shown in Figure 2 (a), it consists of a graph-attention layer [53] followed by temporal convolution and a linear layer. The graph attention layer helps in learning the weighted accumulation of features from all the EEG channels into a common representation. Then we apply temporal convolution and feature projection to get  $\psi \in \mathbb{R}^{1024}$  dimension feature.

#### 3.2. EEG Features to Video Frames

To synthesize video frames from learned EEG representation, we follow the work of [46] and use StyleGAN-ADA [18] architecture as shown in Figure 2 (b). We train the EEGStyleGAN-ADA [46] from scratch with a modification

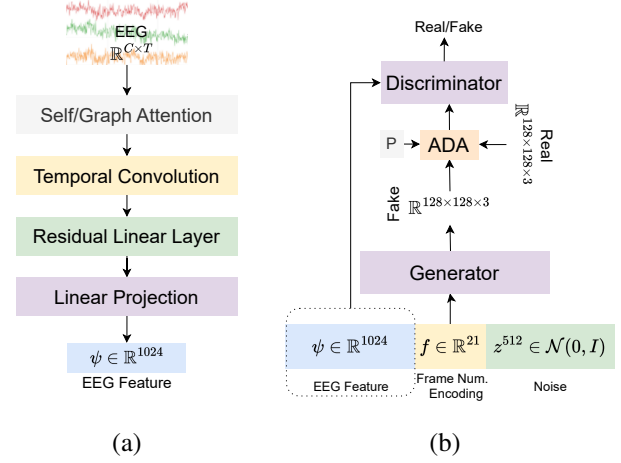


Figure 2. The figure illustrates the EEG-Video framework. (a) Modified NICE EEG [47] network used for encoding the EEG into the representation space. (b) The StyleGAN-ADA [18] based network for synthesizing video frames from learned EEG representation. Here, along with EEG features, we have also encoded the frame number to synthesize particular frames in the video.

to the conditioning input because the GAN network under consideration is designed for image synthesis only. To generate video frames using EEG signal, as shown in Figure 2, we concatenated positionally encoded frame number ( $f$ ), *i.e.*, temporal information of video with EEG features following [37]. We have used sinusoidal positional encoding [52] to encode frame numbers. The concatenation of frame encoding gives us control over the different frames associated with the same EEG feature, allowing temporally conditioned frame synthesis. We also modified the generator loss [18] to include  $L_1$  loss with the ground truth frame with weights  $\lambda_1 = 0.5$  and  $\lambda_2 = 5.0$ . Figure 1 shows visual differences between frames; Table 1 quantifies the quality of synthesized frames.

$$\mathcal{L}_{total}^{Gen} = \lambda_1 * \mathcal{L}_{Gen} + \lambda_2 * \mathcal{L}_1(Gen, Real) \quad (2)$$

### 4. Experiments

In this section, we will discuss a) datasets used for the study, b) the effect of different label classes for extracting features from EEG data across different datasets using triplet loss, c) how much information different brain regions contain for dynamic visual stimuli and d) synthesizing video frames from EEGStyleGAN-ADA [46] network. This section aims to explore how much information about different activities EEG stores. For all the empirical studies, we follow the following: the input to the neural network is EEG of shape  $\mathbb{R}^{c \times t}$  where  $c$  is the channel number,  $t$  is the total number of time samples, and the output of the network is a unit normalized feature of shape  $\mathbb{R}^{1024}$ . The evaluation is done using

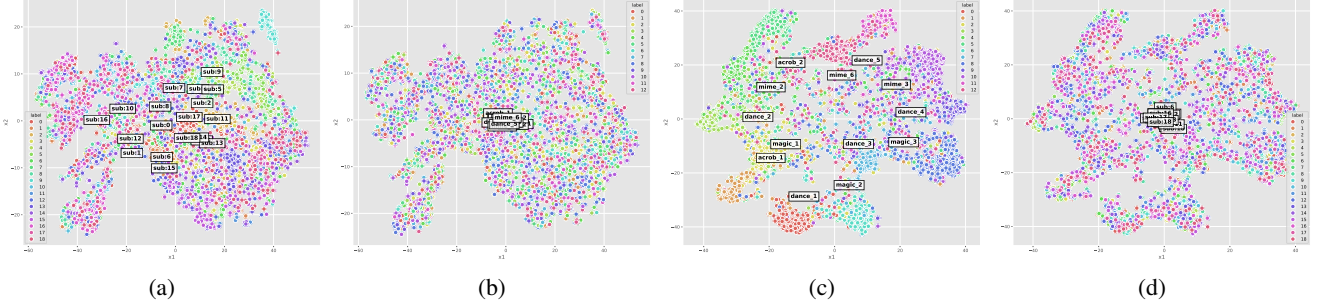


Figure 3. **Effect of Triplet Loss.** The figure illustrates four different t-SNE [51] plots to show the effect of how triplet loss aligned EEG feature space based on the label it trained for. We extracted the feature from random weights initialized EEG encoder and plotted a *t*-SNE map for (a) subject label (19 subjects) and (b) video label (13 videos). As shown, EEG features are able to cluster the subject up to some accuracy (18 – 20%, *k*-means accuracy) and form a single cluster (8 – 9% *k*-means accuracy) for video features. On the contrary, when the EEG encoder is trained using triplet loss over video labels, (c) it forms different clusters for different video classes ( 70% *k*-means accuracy), but (d) forms a single cluster for subject classes ( 8% *k*-means accuracy). The study is performed over the Video-EEG Action dataset [59].

Dataset	Model	LPIPS (↓)	PSNR (↑)	SSIM (↑)
SEED [10, 64]	Ours	0.587	10.799	0.153
EEG-Video Action [59]	Ours	0.418	16.220	0.431
SEED-DV [28]	EEG2Video [28]	-	-	0.256
	Ours	0.6898	9.6151	0.1434

Table 1. Quantitative evaluation of modified EEGStyleGAN-ADA [46] for video frame generation.

*k*-means [14] classification accuracy. The implementation details are shared in the supplementary material.

#### 4.1. Datasets

We have used two different EEG-Video datasets for the proposed study. The first one is the SEED (SJTU Emotion EEG Dataset) [10, 64], which is an emotion-based dataset. It consists of EEG recordings from 15 participants (7 males and 8 females), collected over three separate sessions spaced approximately one week apart. During each session, participants watched 15 video clips, each lasting around four minutes, selected to induce three emotional states: positive, neutral, and negative. EEG signals were recorded using a 62-channel ESI NeuroScan System [33].

The second dataset we have used is the Video-EEG Action dataset [59]. It is designed to explore the neural representation of natural single-shot videos in the human brain using electroencephalogram (EEG) recordings. The dataset comprises EEG data collected from 19 participants with normal or corrected-to-normal vision while they watched a set of 13 muted YouTube videos. EEG signals were recorded using a 64-channel BioSemi ActiveTwo [3] system at a sampling rate of 2048 Hz.

Apart from the above two datasets, we have also done the study on the SEED-DV [28] dataset. It consists of 20 subjects recording when viewing 1400 video clips across 40 different classes. All the empirical studies on SEED-DV are presented in the supplementary.

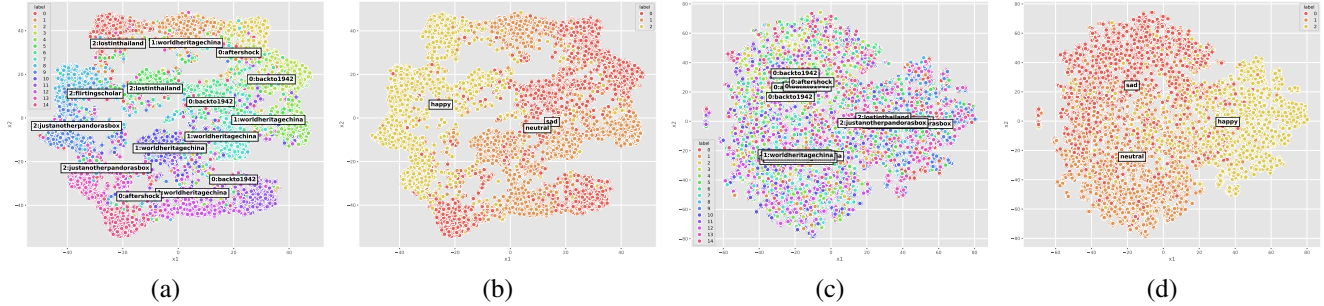
#### 4.2. Pre-processing EEG Datasets

For the SEED dataset, we directly used the pre-processed EEG signals released by the authors, containing EEG signals downsampled to 200Hz with a band-pass filter applied from 0 – 75Hz. For the Video-EEG action dataset, we followed similar pre-processing steps for EEG (except for downsampling) as in [59]: a) interpolate bad channels, b) re-reference the data to average, c) apply a notch filter to remove line noise, d) apply high pass frequency filter with a high-pass cutoff of 0.5Hz. e) downsample EEG data to 200Hz, and f) regress out the Electrooculography (EOG) channels to remove artifacts due to eye movements.

We chunked the EEG and corresponding video for both datasets into 2-second segments with no overlap, resulting in EEG segments of 400-time points each. We created the segments for each video in a way that 80% of the segments from each video are in the train split, 10% in the validation split, and 10% in the test split. The distribution of the segments among the train, validation, and test splits was done randomly. For experiments following, leave-two-subject-out, all segments of the last two subjects were in the test split (subjects 14 and 15 for the SEED dataset and subjects 18 and 19 for the Video-EEG action dataset), and the remaining segments were in the train split.

#### 4.3. What does an EEG encode?

We perform empirical studies on both datasets to understand how effective triplet loss [41] is while learning meaningful representation for EEG signals. We first performed a study on the EEG Video-Action dataset [59], where we extracted the EEG signal features from the randomly initialized neural network. The extracted features are then clustered over the subject labels and video classes. As shown in Figure 3 (a), the subject’s clusters are well spread out without training; this shows EEG’s inherent information about



subject identity. The cluster observed for video classes Figure 3 (b) is not well spread out, showing the extracted features don't hold much information about the videos compared to subject information. Following this, we train the network on video labels using triplet loss. Figure 3 (c) shows that features from EEG signals, when trained with video labels, can encode the information that discriminates between EEGs from different video stimuli. When we try to cluster the learned EEG representation over the subject ID, it collapses to one cluster, as shown in Figure 3 (d). This confirms that triplet loss helps the network to extract meaningful features from EEG signals based on the given labels.

The SEED dataset consists of both emotion as well as video class labels as described in Section 4.2. In this case, we train the feature extraction network on both labels. Figure 4 (a-b) shows the clustering of video labels and subject labels when the feature extraction network is trained using video labels. The network is able to extract information about video stimuli from the EEG signals, and it clusters the video based on it. Interestingly, when the features are clustered over emotions, it aligns well with the video. In contrast, when we train the network on the emotion labels and do the clustering as shown in Figure 4 (c), the features are not able to discriminate between different video stimuli and form clusters based on emotion labels only Figure 4 (d).

#### 4.4. How does a Brain Region affect EEG Signals?

In this study, we investigated the classification performance of EEG signals across different brain regions for two distinct tasks: video classification (15 classes) for both SEED [10, 64] as well as Video-EEG Action [59] datasets, and emotion classification (3 classes) only for the SEED dataset. First, the EEG feature extraction network is trained using only region-specific EEG channels. Then the results were evaluated under two experimental regimes: *R1*) All Subject, where training, validation, and testing were performed on non-overlapping epochs of the same subjects, and *R2*)

Leave Two Subjects, where the model was trained on  $S - 2$  subjects and tested on two unseen subjects (subjects  $S - 1$  and  $S$ ), where  $S$  is the total number of subjects present in the dataset.

**Video Classification on SEED Dataset.** The first experiment focused on classifying video stimuli into 15 categories using all the channels of EEG signals. Under the All Subject regime, the model achieved an overall accuracy of 66.84%, which is significantly higher than the chance level of 6.67%, demonstrating that EEG signals encode meaningful information related to video stimuli as shown in the first row of Figure 5. We further investigate how much information the different brain regions have about the video stimuli. To study this, as shown in Figure [5, 7], we divide the brain region into chunks, i.e., we sample the channel from the EEG dataset based on this division of the brain region. The observations are as follows: a) A hemispheric asymmetry was observed, with the Left Hemisphere achieving significantly higher accuracy (54.39%) compared to the Right Hemisphere (28.32%). b) The Front Region outperformed the Back Region (31.21% vs. 26.65%), indicating that frontal areas play a critical role in attention and decision-making during dynamic stimuli processing.

To evaluate generalization across subjects, we conducted video classification under the Leave Two Subjects regime. The overall accuracy dropped to 19.09%, highlighting challenges in cross-subject generalization due to inter-individual variability in EEG patterns. Figure 7 shows hemispheric asymmetry persisted, with the Left Hemisphere outperforming the Right Hemisphere (19.33% vs. 16.43%).

**Emotion Classification on SEED Dataset.** The second experiment focused on emotion classification into three categories (positive, neutral, and negative). Under the All Subject regime, the model achieved an impressive overall accuracy of 76.33%, well above the chance level (33.33%), indicating that EEG signals are highly discriminative for

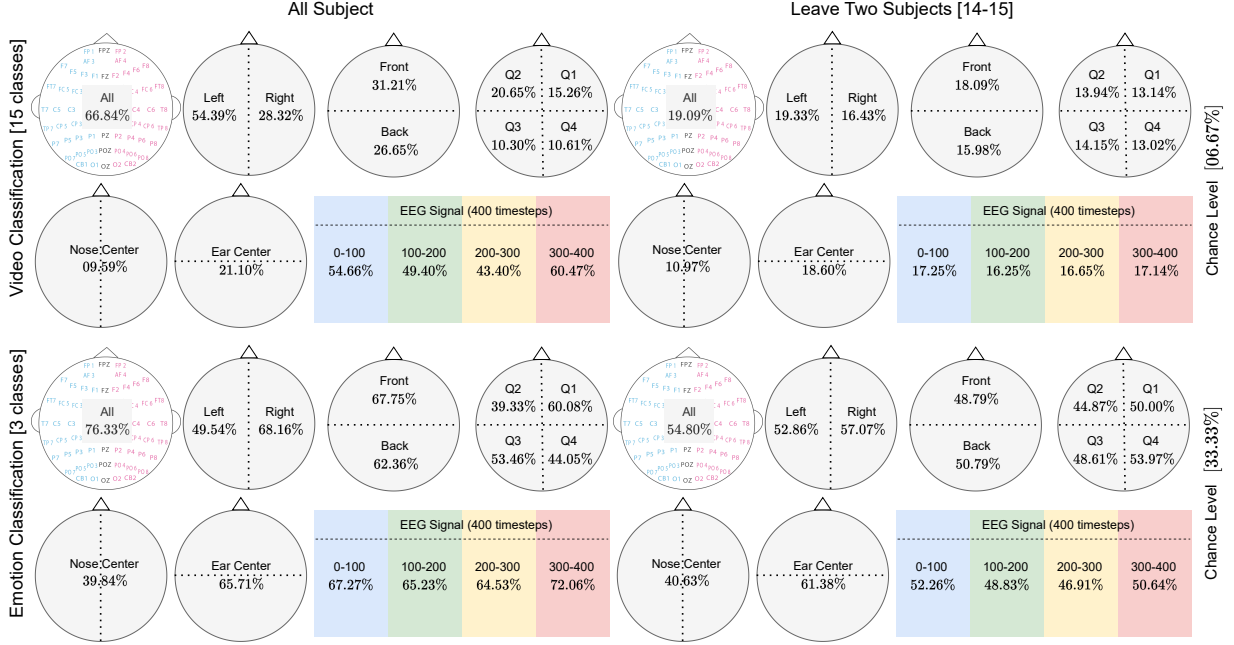


Figure 5. **Vision-Emotion Decoding SEED Dataset.** The figure shows the test classification accuracy of EEG signals when trained on different brain region channels across two different tasks: video classification and emotion classification on the SEED dataset [10, 64]. Two columns represent two different experimental regimes for evaluation. In all subjects, the train-val-test sampled from the same epoch of the EEG ensures a non-overlapping region. In leaving two subjects, the network is trained on the data of subjects from 1 – 13 and tested on subjects 14 and 15 from the SEED dataset. To show the effect of different non-overlapping time segments in the case of a pre-trained network, we mask a particular timestep and calculate the accuracy considering all the EEG channels.

emotional states. The brain region observations are as follows: a) Unlike video classification, emotion classification exhibited a dominance of the Right Hemisphere, which achieved significantly higher accuracy (68.16%) compared to the Left Hemisphere (49.54%). b) The front Region is better than the Back Region (67.75% vs. 62.36%), reflecting the role of prefrontal areas in emotion regulation and cognitive appraisal. In the work by Liu *et al* [27] achieves 87.03% accuracy in emotion classification on the SEED dataset, given our focus on visual reconstruction, we do not optimize specifically for emotion decoding. Our objective is to extract visual features and analyze the information content over different regions and throughout time, rather than achieving state-of-the-art in emotion recognition.

Under the leave two-subject regime, emotion classification showed better generalization compared to video classification but still experienced a notable drop in performance, achieving an overall accuracy of 54.80%. The Right Hemisphere remained dominant over the Left Hemisphere (57.07% vs. 52.86%), reinforcing its critical role in emotional processing.

#### Video Classification on EEG-Video Action Dataset.

Figure 6 shows the classification performance of EEG signals for video decoding tasks using the EEG-Video Action Dataset [59]. The model achieves an accuracy of 56.83%

for video classification across 13 classes, significantly above the chance level (7.69%) in the All Subject regime. The Left Hemisphere outperforms the Right Hemisphere, achieving an accuracy of 44.73% compared to 31.89%, suggesting left-lateralized processing for structured visual interpretation tasks, which confirms the above findings from the SEED dataset. But contrary to the SEED dataset study, the Back Region performs better (46.91%) than the Front Region (37.34%), indicating that posterior regions, particularly posterior parietal areas, play a dominant role in decoding visual stimuli due to their involvement in early visual processing given that the EEG-Video Action dataset does not contain emotion heavy videos stimuli and mostly involves action related motions. It aligned with the existing study that found the activation in the posterior parietal lobe during the observation of object-based actions [5].

In the case of Leave Two Subject regime, the accuracy drops to 22.38%, highlighting challenges in generalizing across subjects due to inter-individual variability in EEG patterns. The Left Hemisphere still outperforms the Right Hemisphere (21.80% vs. 15.47%), consistent with findings from the All Subject regime and the above study over the SEED dataset.

**Effect of Different Brain Lobes.** To study the effect of how different brain lobes process the information from

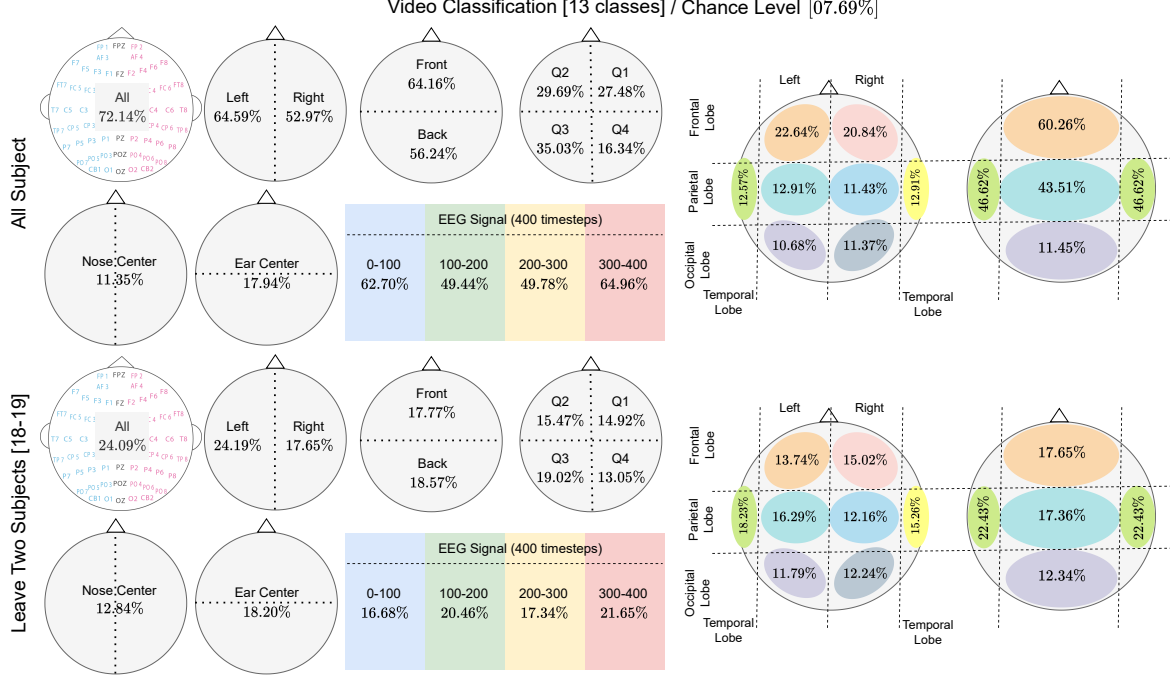


Figure 6. **Video Decoding EEG-Video Action Dataset.** The figure illustrates the effect of sampling EEG channels from specific brain regions and performing training and testing of the EEG feature extraction network over the video labels from the EEG-Video Action dataset [59]. It also shows the effect of different non-overlapping time segments in the pre-trained networks with all the channels, i.e., what will be the effect on classification when we mask a particular region of time ( $t_1-t_2$ )?

video stimuli, we filter the EEG channels from those regions to train-test the classification accuracy as shown in Figure [6, 7]. The region highlighted in the figures for different lobes is approximated, and the accurate EEG channel maps are shown in the supplementary. Across both the datasets SEED [10, 64] and EEG-Video Action [59], the temporal lobe has the highest classification accuracy, including all the regimes. For emotion-based classification, the partial lobe has the highest accuracy apart from the temporal lobe.

**Temporal Dynamics.** In the Figures [5, 6] we show the effect of timesteps in the case of a pre-trained EEG network for the video classification task and emotion task in the case of the SEED dataset. We first train the network for classification tasks, which can be based on the video or the emotion label. Once the network is trained, while performing the inference, we mask the EEG timesteps between  $t_1$  and  $t_2$  and extract the features for the masked EEG. The  $k$ -means [14] classification is performed over these masked EEG features. Across all the empirical studies for video stimuli, the EEG has a significant drop in accuracy between timesteps 100 – 300.

#### 4.5. Can we reconstruct Dynamic Visual Stimulus from EEG Signals?

To address this question, we train an EEGStyleGAN-ADA [46] network for video frame generation conditioned over

the extracted features from EEG signals when trained for the video discrimination task using triplet loss following Regime-1 from the experiment section. For the video synthesis task, we sampled four frames distributed across time and paired them with the EEG signal. Figure 1 shows the synthesis result on the SEED dataset, and it shows that the generated frames closely align with the video stimuli shown to the participants. We observed similar outcomes in the case of the Action dataset, as shown in Figure 1. We have also evaluated the generated results over three different metrics, i.e., LPIPS [63], PSNR [17], and SSIM [56] as shown in Table 1.

## 5. Discussion

This work addresses the problem of dynamic visual reconstruction from the EEG signals. To achieve that, we need to extract meaningful features from EEG signals. For our study, we used the SEED [10, 64] dataset, which is an emotion response EEG recording when participants are watching emotional videos, and the EEG-Video Action [59] dataset, which is a recording of participants watching action-based videos. Our *All Subject* split uses non-overlapping segments from each video. The *Leave-Two-Subject* regime (subjects 14–15 in SEED, 18–19 in Action) further verifies generalization (Figure 6-7), mitigating con-

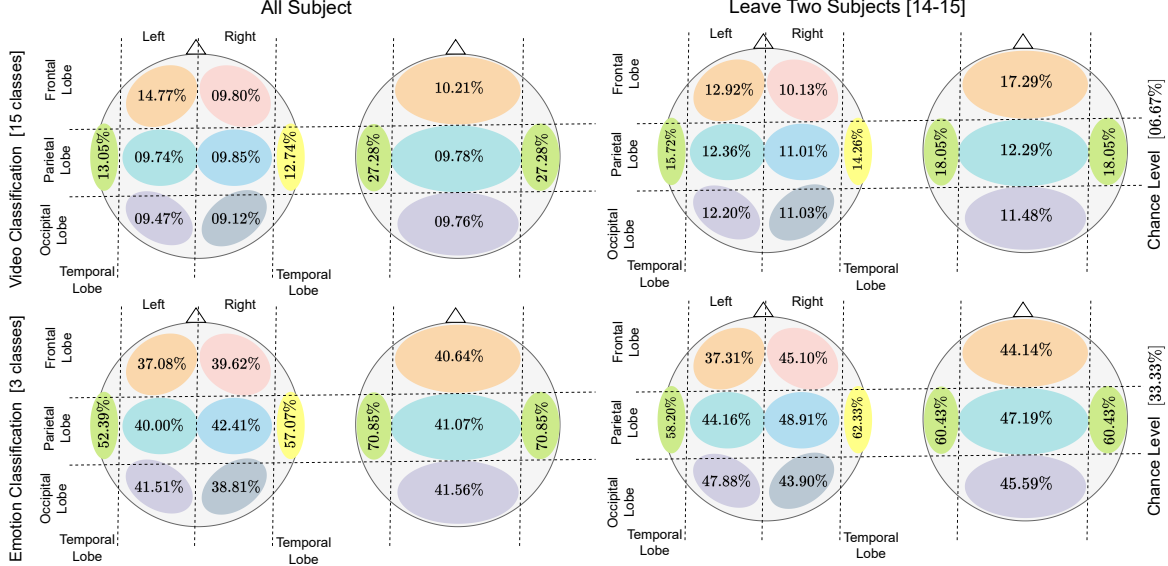


Figure 7. **Brain Lobe Region.** To show how much information about video and emotion is processed from each brain lobe region, we selected the channels specifically from those regions based on the SEED dataset [10, 64] EEG channel map to perform training and testing. Two columns represent two different experimental regimes for evaluation. In all subjects, the train-val-test sampled from the same epoch of the EEG ensures non-overlapping segments. In leaving two subjects, the network is trained on the data of subjects from 1 – 13 and tested on subjects 14 and 15 from the SEED dataset.

cerns about within-video correlation or leakage.

The video generation study focuses on synthesizing dynamic visual information from EEG signals. For this, we extracted the features from a pre-trained EEG video classification network and trained a modified EEGStyleGAN-ADA [46] for video frame synthesis by adding temporal encoding that enables the generator to map EEG features to specific video frame positions. The temporal encoding provides the temporal context necessary for dynamic vision reconstruction. *Our goal is not merely to improve video synthesis quality, but to probe the extent to which the temporally grounded visual content can be decoded from EEG alone. Unlike works such as EEG2Video [28] that rely on Seq2Seq models or vision-language pretraining, our approach evaluates EEG as a stand-alone modality without leveraging additional information from other modalities.*

The latter part of the study focuses on which brain region contributes more to the information present in EEG signals. For video-based activity, the outcome suggests the left hemisphere has more visual processing information than the emotion-based activity, where the right hemisphere has shown high activity. Further, we studied the importance of the timestep from EEG signals, analysis in Figures 6–7 reveals that EEG timesteps 100–300 encode the most dynamic visual information. For SEED-DV [28], we performed both triplet learning and a multimodal learning strategy to show how leveraging additional information in the form of text slightly improves the k-means clustering accuracy (please refer to the supplementary).

All the empirical analyses done in the work are tightly coupled to the goal of understanding what types of information the EEG encodes. For example, the t-SNE and clustering experiments in Figure 3–4 reveal how emotional and visual representations manifest in EEG, which directly informs how reliably these signals support video reconstruction.

## 6. Conclusion

In this work, we present a thorough study and a comprehensive framework for synthesizing dynamic visual stimuli from EEG signals. Our method generates eight video frames from EEG signals of shape  $128 \times 128$  by modifying the conditioning of the EEGStyleGAN-ADA network. We benchmark the generated frames using visual quality metrics, evaluating their similarity to the original stimuli shown to participants during EEG recording. In addition to frame synthesis, we conduct extensive empirical studies to assess the effectiveness of triplet loss for feature extraction using class labels. The dataset employed in this study contains both emotion-based and video-based class labels, allowing us to analyze the significance of different brain regions. Our findings reveal that the left hemisphere predominantly encodes visual processing information, while the right hemisphere exhibits stronger emotional responses, corroborating established research in neuroscience. We believe that the insights gained here will inspire future research in the reconstruction of dynamic visual stimuli from EEG signals.

## 7. Acknowledgement

This work is supported by the Prime Minister Research Fellowship (PMRF2122-2557) and the Jibaben Patel Chair in Artificial Intelligence.

## References

- [1] Roman Beliy, Guy Gaziv, Assaf Hoogi, Francesca Strappini, Tal Golan, and Michal Irani. From voxels to pixels and back: Self-supervision in natural-image reconstruction from fmri. *Advances in Neural Information Processing Systems*, 32, 2019. 2
- [2] Yohann Benchetrit, Hubert Banville, and Jean-Rémi King. Brain decoding: toward real-time reconstruction of visual perception. *arXiv preprint arXiv:2310.19812*, 2023. 2
- [3] BioSemi. ActiveTwo EEG System. <https://www.biosemi.com>. Accessed: 2025-03-06. 4
- [4] Gijs Joost Brouwer and David J Heeger. Decoding and reconstructing color from responses in human visual cortex. *Journal of Neuroscience*, 29(44):13992–14003, 2009. 2
- [5] Giovanni Buccino, Ferdinand Binkofski, Gereon R Fink, Luciano Fadiga, Leonardo Fogassi, Vittorio Gallese, Rüdiger J Seitz, Karl Zilles, Giacomo Rizzolatti, and H-J Freund. Action observation activates premotor and parietal areas in a somatotopic manner: an fmri study. *European journal of neuroscience*, 13(2):400–404, 2001. 2, 6
- [6] Randy L Buckner. Event-related fmri and the hemodynamic response. *Human brain mapping*, 6(5-6):373–377, 1998. 2
- [7] Zijiao Chen, Jiaxin Qing, Tiange Xiang, Wan Lin Yue, and Juan Helen Zhou. Seeing beyond the brain: Conditional diffusion model with sparse masked modeling for vision decoding. In *Proceedings of the IEEE/CVF Conference on Computer Vision and Pattern Recognition*, pages 22710–22720, 2023. 2
- [8] Zijiao Chen, Jiaxin Qing, and Juan Helen Zhou. Cinematic mindscapes: High-quality video reconstruction from brain activity. *Advances in Neural Information Processing Systems*, 36:24841–24858, 2023. 2, 3
- [9] Corinna Cortes and Vladimir Vapnik. Support-vector networks. *Machine learning*, 20:273–297, 1995. 1
- [10] Ruo-Nan Duan, Jia-Yi Zhu, and Bao-Liang Lu. Differential entropy feature for eeg-based emotion classification. In *2013 6th international IEEE/EMBS conference on neural engineering (NER)*, pages 81–84. IEEE, 2013. 1, 4, 5, 6, 7, 8, 2, 3
- [11] William Fish. *Philosophy of perception: A contemporary introduction*. Routledge, 2021. 2
- [12] Camilo Fosco, Benjamin Lahner, Bowen Pan, Alex Andonian, Emilie Josephs, Alex Lascelles, and Aude Oliva. Brain netflix: Scaling data to reconstruct videos from brain signals. In *European Conference on Computer Vision*, pages 457–474. Springer, 2024. 2, 3
- [13] Guy Gaziv, Roman Beliy, Niv Granot, Assaf Hoogi, Francesca Strappini, Tal Golan, and Michal Irani. Self-supervised natural image reconstruction and large-scale semantic classification from brain activity. *NeuroImage*, 254: 119121, 2022. 2
- [14] John A Hartigan and Manchek A Wong. Algorithm as 136: A k-means clustering algorithm. *Journal of the royal statistical society. series c (applied statistics)*, 28(1):100–108, 1979. 4, 7
- [15] Alexander Hepburn, Valero Laparra, Jesús Malo, Ryan McConville, and Raul Santos-Rodriguez. Perceptnet: A human visual system inspired neural network for estimating perceptual distance. In *2020 IEEE International Conference on Image Processing (ICIP)*, pages 121–125. IEEE, 2020. 2
- [16] Jonathan Ho, Ajay Jain, and Pieter Abbeel. Denoising diffusion probabilistic models. *Advances in neural information processing systems*, 33:6840–6851, 2020. 2
- [17] A. Hore and D. Ziou. Image quality metrics: Psnr vs. ssim. *20th International Conference on Pattern Recognition*, pages 2366–2369, 2010. 7
- [18] Tero Karras, Miika Aittala, Janne Hellsten, Samuli Laine, Jaakko Lehtinen, and Timo Aila. Training generative adversarial networks with limited data. *Advances in neural information processing systems*, 33:12104–12114, 2020. 3, 1
- [19] Isaak Kavasidis, Simone Palazzo, Concetto Spampinato, Daniela Giordano, and Mubarak Shah. Brain2image: Converting brain signals into images. In *Proceedings of the 25th ACM international conference on Multimedia*, pages 1809–1817, 2017. 2
- [20] Gwanghyun Kim, Taesung Kwon, and Jong Chul Ye. Diffusionclip: Text-guided diffusion models for robust image manipulation. In *Proceedings of the IEEE/CVF conference on computer vision and pattern recognition*, pages 2426–2435, 2022. 2
- [21] Diederik P Kingma. Adam: A method for stochastic optimization. *arXiv preprint arXiv:1412.6980*, 2014. 1
- [22] George H Klem. The ten-twenty electrode system of the international federation. the international federation of clinical neurophysiology. *Electroencephalogr. Clin. Neurophysiol. Suppl.*, 52:3–6, 1999. 2
- [23] Stephen M Kosslyn. A cognitive neuroscience of visual cognition: Further developments. In *Advances in psychology*, pages 351–381. Elsevier, 1991. 2
- [24] Ganit Kupersmidt, Roman Beliy, Guy Gaziv, and Michal Irani. A penny for your (visual) thoughts: Self-supervised reconstruction of natural movies from brain activity. *arXiv preprint arXiv:2206.03544*, 2022. 2
- [25] Victor Weixin Liang, Yuhui Zhang, Yongchan Kwon, Serena Yeung, and James Y Zou. Mind the gap: Understanding the modality gap in multi-modal contrastive representation learning. *Advances in Neural Information Processing Systems*, 35:17612–17625, 2022. 2
- [26] Sikun Lin, Thomas Sprague, and Ambuj K Singh. Mind reader: Reconstructing complex images from brain activities. *Advances in Neural Information Processing Systems*, 35:29624–29636, 2022. 2
- [27] Xucheng Liu, Ting Li, Cong Tang, Tao Xu, Peng Chen, Anastasios Bezerianos, and Hongtao Wang. Emotion recognition and dynamic functional connectivity analysis based on eeg. *IEEE Access*, 7:143293–143302, 2019. 6
- [28] Xuan-Hao Liu, Yan-Kai Liu, Yansen Wang, Kan Ren, Hanwen Shi, Zilong Wang, Dongsheng Li, Bao-Liang Lu, and

- Wei-Long Zheng. Eeg2video: Towards decoding dynamic visual perception from eeg signals. *Advances in Neural Information Processing Systems*, 37:72245–72273, 2025. 1, 2, 4, 8, 5, 7
- [29] Lu Meng and Chuanhao Yang. Semantics-guided hierarchical feature encoding generative adversarial network for visual image reconstruction from brain activity. *IEEE Transactions on Neural Systems and Rehabilitation Engineering*, 32:1267–1283, 2024. 2
- [30] Rahul Mishra and Arnav Bhavsar. Eeg classification for visual brain decoding via metric learning. In *BIOIMAGING*, pages 160–167, 2021. 3
- [31] Yoichi Miyawaki, Hajime Uchida, Okito Yamashita, Masaaki Sato, Yusuke Morito, Hiroki C Tanabe, Norihiro Sadato, and Yukiyasu Kamitani. Visual image reconstruction from human brain activity using a combination of multiscale local image decoders. *Neuron*, 60(5):915–929, 2008. 2
- [32] Thomas Naselaris, Ryan J Prenger, Kendrick N Kay, Michael Oliver, and Jack L Gallant. Bayesian reconstruction of natural images from human brain activity. *Neuron*, 63(6):902–915, 2009. 2
- [33] Compumedics NeuroScan. *ESI NeuroScan System*. Compumedics Ltd., Charlotte, NC, USA, Accessed 2025. Available: <https://www.compumedics.com.au/products/neuroscan/>. 4
- [34] Furkan Ozelcik and Rufin VanRullen. Natural scene reconstruction from fmri signals using generative latent diffusion. *Scientific Reports*, 13(1):15666, 2023. 2
- [35] Furkan Ozelcik, Bhavin Choksi, Milad Mozafari, Leila Reddy, and Rufin VanRullen. Reconstruction of perceived images from fmri patterns and semantic brain exploration using instance-conditioned gans. In *2022 international joint conference on neural networks (IJCNN)*, pages 1–8. IEEE, 2022. 2
- [36] Simone Palazzo, Concetto Spampinato, Isaak Kavasidis, Daniela Giordano, and Mubarak Shah. Generative adversarial networks conditioned by brain signals. In *Proceedings of the IEEE international conference on computer vision*, pages 3410–3418, 2017. 2
- [37] Albert Pumarola, Enric Corona, Gerard Pons-Moll, and Francesc Moreno-Noguer. D-nerf: Neural radiance fields for dynamic scenes. In *Proceedings of the IEEE/CVF conference on computer vision and pattern recognition*, pages 10318–10327, 2021. 3
- [38] Alec Radford, Jong Wook Kim, Chris Hallacy, Aditya Ramesh, Gabriel Goh, Sandhini Agarwal, Girish Sastry, Amanda Askell, Pamela Mishkin, Jack Clark, et al. Learning transferable visual models from natural language supervision. In *International conference on machine learning*, pages 8748–8763. PmLR, 2021. 2, 3, 1
- [39] Robin Rombach, Andreas Blattmann, Dominik Lorenz, Patrick Esser, and Björn Ommer. High-resolution image synthesis with latent diffusion models. In *Proceedings of the IEEE/CVF conference on computer vision and pattern recognition*, pages 10684–10695, 2022. 2
- [40] Sanne Schoenmakers, Markus Barth, Tom Heskes, and Marcel Van Gerven. Linear reconstruction of perceived images from human brain activity. *NeuroImage*, 83:951–961, 2013. 2
- [41] Florian Schroff, Dmitry Kalenichenko, and James Philbin. Facenet: A unified embedding for face recognition and clustering. In *Proceedings of the IEEE conference on computer vision and pattern recognition*, pages 815–823, 2015. 3, 4, 1
- [42] Johannes Schultz and Karin S Pilz. Natural facial motion enhances cortical responses to faces. *Experimental brain research*, 194(3):465–475, 2009. 2
- [43] Paul Scotti, Atmadeep Banerjee, Jimmie Goode, Stepan Shabalín, Alex Nguyen, Aidan Dempster, Nathalie Verlinde, Elad Yundler, David Weisberg, Kenneth Norman, et al. Reconstructing the mind’s eye: fmri-to-image with contrastive learning and diffusion priors. *Advances in Neural Information Processing Systems*, 36:24705–24728, 2023. 2
- [44] Paul S Scotti, Mihir Tripathy, Cesar Kadir Torrico Villanueva, Reese Kneeland, Tong Chen, Ashutosh Narang, Charan Santhirasegaran, Jonathan Xu, Thomas Naselaris, Kenneth A Norman, et al. Mindeye2: Shared-subject models enable fmri-to-image with 1 hour of data. *arXiv preprint arXiv:2403.11207*, 2024. 2
- [45] Prajwal Singh, Pankaj Pandey, Krishna Miyapuram, and Shanmuganathan Raman. Eeg2image: Image reconstruction from eeg brain signals. In *ICASSP 2023-2023 IEEE International Conference on Acoustics, Speech and Signal Processing (ICASSP)*, pages 1–5. IEEE, 2023. 3, 1
- [46] Prajwal Singh, Dwip Dalal, Gautam Vashishtha, Krishna Miyapuram, and Shanmuganathan Raman. Learning robust deep visual representations from eeg brain recordings. In *Proceedings of the IEEE/CVF Winter Conference on Applications of Computer Vision*, pages 7553–7562, 2024. 3, 4, 7, 8
- [47] Yonghao Song, Bingchuan Liu, Xiang Li, Nanlin Shi, Yijun Wang, and Xiaorong Gao. Decoding natural images from eeg for object recognition. *arXiv preprint arXiv:2308.13234*, 2023. 3, 1
- [48] Jingyuan Sun, Mingxiao Li, Zijiao Chen, Yunhao Zhang, Shaonan Wang, and Marie-Francine Moens. Contrast, attend and diffuse to decode high-resolution images from brain activities. *Advances in Neural Information Processing Systems*, 36:12332–12348, 2023. 2
- [49] Jingyuan Sun, Mingxiao Li, Zijiao Chen, and Marie-Francine Moens. Neurocine: Decoding vivid video sequences from human brain activities, 2024. 2, 3
- [50] Yu Takagi and Shinji Nishimoto. High-resolution image reconstruction with latent diffusion models from human brain activity. In *Proceedings of the IEEE/CVF Conference on Computer Vision and Pattern Recognition*, pages 14453–14463, 2023. 2
- [51] Laurens Van der Maaten and Geoffrey Hinton. Visualizing data using t-sne. *Journal of machine learning research*, 9 (11), 2008. 4
- [52] Ashish Vaswani, Noam Shazeer, Niki Parmar, Jakob Uszkoreit, Llion Jones, Aidan N Gomez, Łukasz Kaiser, and Illia Polosukhin. Attention is all you need. *Advances in neural information processing systems*, 30, 2017. 3

- [53] Petar Veličković, Guillem Cucurull, Arantxa Casanova, Adriana Romero, Pietro Lio, and Yoshua Bengio. Graph attention networks. *arXiv preprint arXiv:1710.10903*, 2017. [3](#)
- [54] Brian A Wandell. Computational neuroimaging of human visual cortex. *Annual review of neuroscience*, 22(1):145–173, 1999. [2](#)
- [55] Chong Wang, Hongmei Yan, Wei Huang, Jiyi Li, Yuting Wang, Yun-Shuang Fan, Wei Sheng, Tao Liu, Rong Li, and HuaFu Chen. Reconstructing rapid natural vision with fmri-conditional video generative adversarial network. *Cerebral Cortex*, 32(20):4502–4511, 2022. [2](#)
- [56] Zhou Wang, Alan C. Bovik, Hamid R. Sheikh, and Eero P. Simoncelli. Image quality assessment: From error visibility to structural similarity. *IEEE Transactions on Image Processing*, 13(4):600–612, 2004. [7](#)
- [57] Haiguang Wen, Junxing Shi, Yizhen Zhang, Kun-Han Lu, Jiayue Cao, and Zhongming Liu. Neural encoding and decoding with deep learning for dynamic natural vision. *Cerebral cortex*, 28(12):4136–4160, 2018. [2](#)
- [58] Weihao Xia, Raoul De Charette, Cengiz Oztireli, and Jing-Hao Xue. Dream: Visual decoding from reversing human visual system. In *Proceedings of the IEEE/CVF Winter Conference on Applications of Computer Vision*, pages 8226–8235, 2024. [2](#)
- [59] Yuanyuan Yao, Axel Stebner, Tinne Tuytelaars, Simon Geirnaert, and Alexander Bertrand. Identifying temporal correlations between natural single-shot videos and eeg signals. *Journal of Neural Engineering*, 21(1):016018, 2024. [1](#), [4](#), [5](#), [6](#), [7](#), [2](#), [3](#)
- [60] Ilker Yildirim, Jiajun Wu, Nancy Kanwisher, and Joshua Tenenbaum. An integrative computational architecture for object-driven cortex. *Current Opinion in Neurobiology*, 55: 73–81, 2019. Machine Learning, Big Data, and Neuroscience. [2](#)
- [61] Matthew D Zeiler and Rob Fergus. Visualizing and understanding convolutional networks. In *Computer Vision—ECCV 2014: 13th European Conference, Zurich, Switzerland, September 6–12, 2014, Proceedings, Part I 13*, pages 818–833. Springer, 2014. [2](#)
- [62] Bohan Zeng, Shanglin Li, Xuhui Liu, Sicheng Gao, Xiaolong Jiang, Xu Tang, Yao Hu, Jianzhuang Liu, and Baochang Zhang. Controllable mind visual diffusion model. In *Proceedings of the AAAI Conference on Artificial Intelligence*, pages 6935–6943, 2024. [2](#)
- [63] Richard Zhang, Phillip Isola, Alexei A. Efros, Eli Shechtman, and Oliver Wang. The unreasonable effectiveness of deep features as a perceptual metric. In *IEEE Conference on Computer Vision and Pattern Recognition (CVPR)*, pages 586–595, 2018. [7](#)
- [64] Wei-Long Zheng and Bao-Liang Lu. Investigating critical frequency bands and channels for eeg-based emotion recognition with deep neural networks. *IEEE Transactions on autonomous mental development*, 7(3):162–175, 2015. [1](#), [4](#), [5](#), [6](#), [7](#), [8](#), [2](#), [3](#)

# EEG Vid: Dynamic Vision from EEG Brain Recordings, How much does EEG know?

## Supplementary Material

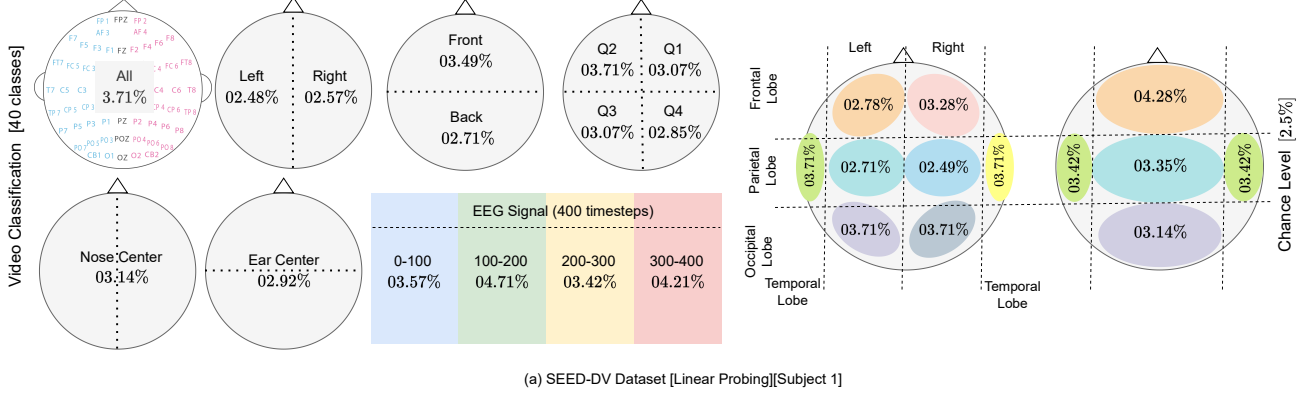


Figure 8. **SEED-DV Brain Region.** The figure illustrates the brain response of subject 1 from the SEED-DV dataset [28]. The EEG channels are sampled from each specific brain region, and representation is learned using a triplet loss-based method. We have reported linear probing accuracy to keep it consistent with findings from the EEG2Video [28].

### A. SEED-DV Experiment

We follow the procedure mentioned in the work [28] for the SEED-DV dataset. We use a triplet-based loss function to extract features from the EEG signal using the proposed feature extraction framework. Triplet loss is conditioned on video classes to enforce learning representation based on the visual stimulus. We follow the 7-fold procedure of [28] to compute the k-mean and linear probing accuracy, where 5 blocks are used for training, 1 block is used for validation, and 1 block is used for reporting the test accuracy. The linear probing is performed to have a fair comparison with the EEG2Video feature extraction method. We train SVM [9] on features learned using our proposed EEG feature extraction framework. Using the GLMNet [28] pipeline, the average accuracy of 20 subjects for 40-way classification of SEED-DV is around 6.20% on raw EEG signals in contrast, we achieve the accuracy of 2.9%, slightly above the chance level of 2.5% and k-means accuracy of 25.6%, owing to feature learned using single modality i.e. only utilizing EEG signals without any pre-trained model. Further, we performed the experiment with multimodal learning where a pre-trained CLIP [38] network is used for text feature extraction, which is available with EEG data, and no modifications to the EEG feature extraction network. We observed a slight improvement in the k-means accuracy 26.3% for 40 classes.

In the Figure 8, we performed the brain region analysis on a single subject (sub1) data from SEED-DV [28]. We follow the k-fold procedure of reporting the accuracy for each brain region. Although the accuracy is slightly

above the chance level, there exists some similarity to the observations found for the SEED dataset in the paper. For example, performance with only the front region is higher compared to the back for both SEED and SEED-DV. Similarly, Q2 has better performance among all the quadrants for both datasets. This indicates the presence of visual information similar to that in the SEED dataset. However, concept-related information is very low, as indicated by a near-chance level accuracy.

### B. Implementation Details

**EEG Feature Extraction.** In this work, the NICE [47] architecture is used as the backbone for EEG feature extraction ( $\psi \in \mathbb{R}^{1024}$ ), which is unit normalized. To train the network, we have used the triplet loss [41] with a multi-similarity miner, which helps learning from hard and semi-hard triplets. We use Adam optimizer [21] with learning rate  $3e-4$  and weight decay  $1e-4$ . The network is trained for 300 epochs.

**EEG Feature to Video.** To synthesize video frames from extracted EEG features, we have used EEGStyleGAN-ADA [45] with modification. The EEGStyleGAN-ADA uses StyleGAN-ADA [18] with modifications to the conditioning network to synthesize the images. We further modified it to condition the temporal frames from video with positional encoding to the EEG features. This helps us synthesize video from an image-based StyleGAN network. We have used sinusoidal positional encoding with encoding dimension as 10 due to better perceptual quality in comparison to lower values.

```

1 import torch
2
3 def encode_position_vectorized(x, enc_dim):
4
5     # Create power vector: [0, 1, 2, ..., enc_dim-1]
6     powers = torch.arange(enc_dim, device=x.device)
7
8     # Calculate frequencies: [2^0, 2^1, 2^2, ..., 2^(enc_dim-1)]
9     frequencies = torch.pow(2.0, powers)
10
11     # Expand dimensions for broadcasting
12     # x shape becomes compatible with frequencies
13     x_expanded = x.unsqueeze(-1)
14
15     # Multiply x by all frequencies at once
16     xf = x_expanded * frequencies
17
18     # Calculate sin and cos for all frequencies simultaneously
19     sin_encodings = torch.sin(xf)
20     cos_encodings = torch.cos(xf)
21
22     # Interleave sin and cos values
23     encodings = torch.stack([sin_encodings, cos_encodings], dim=-1).flatten(-2)
24
25     # Concatenate original x with encodings along the last dimension
26     result = torch.cat([x.unsqueeze(-1), encodings], dim=-1)
27
28     return result
29
30 for eeg_feat, class_id, video_frames_path in x_dataset:
31     eeg_feat = eeg_feat.detach().cpu()
32     for per_frame_idx in range(total_frames):
33         images_path.append(video_frames_path)
34         images_idx.append(per_frame_idx)
35         labels.append(class_id*total_frames+per_frame_idx)
36         temp_eeg_feat =
37         encode_position_vectorized(torch.tensor(per_frame_idx).float(), 10)
38         eeg_feat.append(torch.cat([eeg_feat, temp_eeg_feat], dim=-1))
39
40 eeg_feat = torch.stack(eeg_feat, dim=0).to(torch.float32)
41 labels = torch.from_numpy(np.array(labels)).to(torch.int32)
42 images_idx = torch.from_numpy(np.array(images_idx)).to(torch.int32)

```

Listing 1. Sinusoidal positional encoding

We have trained the GAN network for approximately 5500 epochs for both SEED [10, 64] and EEG-Video Action [59] datasets. For SEED-DV [28], we trained the network for 2500 epochs. The following hyperparameters are used for the training:

```

1 # SEED and EEG-Video Action

```

```

3 'cifar': dict(ref_gpus=1, kimg=5500, mb=32,
               mbstd=8, fmaps=0.75, lrate=0.002, gamma=5,
               ema=20, ramp=0.05, map=8)
4
5 # SEED-DV
6 'cifar': dict(ref_gpus=1, kimg=2500, mb=16,
               mbstd=4, fmaps=1.0, lrate=0.0015, gamma=2,
               ema=10, ramp=0.05, map=4),

```

Listing 2. Hyperparameters for VideoEEGStyleGAN-ADA

## C. Ablation Study

We split the EEGs in the SEED [10, 64] dataset based on the timesteps to study how well the representation learning network generalizes across time. The first 78% of the timesteps are used for training the network. The rest of the split of the EEG dataset 10 – 10%, was used for validation and testing. The 2% EEG samples from training are not included to ensure non-overlap with validation and test. As shown in Figure 9, the study’s findings proposed in the paper hold that visual classification accuracy from the brain’s left hemisphere is more than that of the right hemisphere.

## D. EEG Cap Montage

Figure 10 shows the layout of electrode locations for the EEG-Video Action dataset and the SEED dataset, respectively. Both layout follows the international 10 – 20 [22] standard for placing the electrodes. Below, we have added the dictionary created to select channels based on the location name across different EEG caps.

```

1 EEG_CAP_SEED_V1 = {
2 'all': np.array([1, 2, 3, 4, 5, 6, 7, 8, 9, 10,
                 11, 12, 13, 14, 15, 16, 17, 18, 19, 20, 21,
                 22, 23, 24, 25, 26, 27, 28, 29, 30, 31, 32,
                 33, 34, 35, 36, 37, 38, 39, 40, 41, 42, 43,
                 44, 45, 46, 47, 48, 49, 50, 51, 52, 53, 54,
                 55, 56, 57, 58, 59, 60, 61, 62], dtype=np.int32),
3 'noseback_left': np.array([1, 4, 6, 7, 8, 9, 15,
                             16, 17, 18, 24, 25, 26, 27, 33, 34, 35, 36,
                             42, 43, 44, 45, 51, 52, 53, 58, 59], dtype=np.int32),
4 'noseback_center': np.array([2, 10, 19, 28, 37,
                               46, 54, 60], dtype=np.int32),
5 'noseback_right': np.array([3, 5, 11, 12, 13, 14,
                              20, 21, 22, 23, 29, 30, 31, 32, 38, 39, 40,
                              41, 47, 48, 49, 50, 55, 56, 57, 61, 62],
                              dtype=np.int32),
6 'noseback_Q1_right': np.array([3, 5, 11, 12, 13,
                                 14, 20, 21, 22, 23], dtype=np.int32),
7 'noseback_Q2_left': np.array([1, 4, 6, 7, 8, 9,
                                15, 16, 17, 18], dtype=np.int32),
8 'noseback_Q3_left': np.array([33, 34, 35, 36, 42,
                                43, 44, 45, 51, 52, 53, 58, 59], dtype=np.int32),
9 'noseback_Q4_right': np.array([38, 39, 40, 41,
                                 47, 48, 49, 50, 55, 56, 57, 61, 62], dtype=np.int32),
10 'leftrigh tear_center': np.array([24, 25, 26, 27,
                                    28, 29, 30, 31, 32], dtype=np.int32),

```

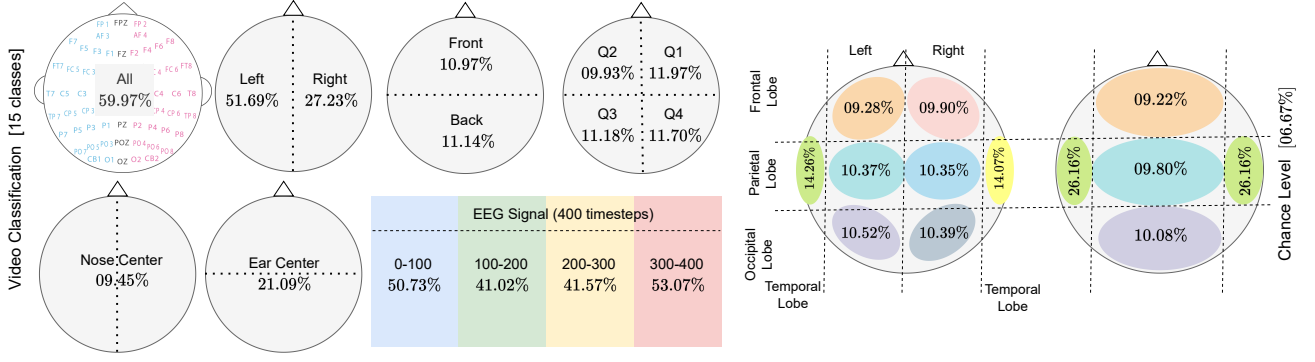


Figure 9. **Ablation.** Figure illustrates the result on SEED dataset [10, 64] when it split based on the timesteps where first 78% steps used for training and last 10 – 10% used for validation and testing making sure non-overlapping segments. As shown in the result the proposed method shows generalizability across the unseen EEG data.

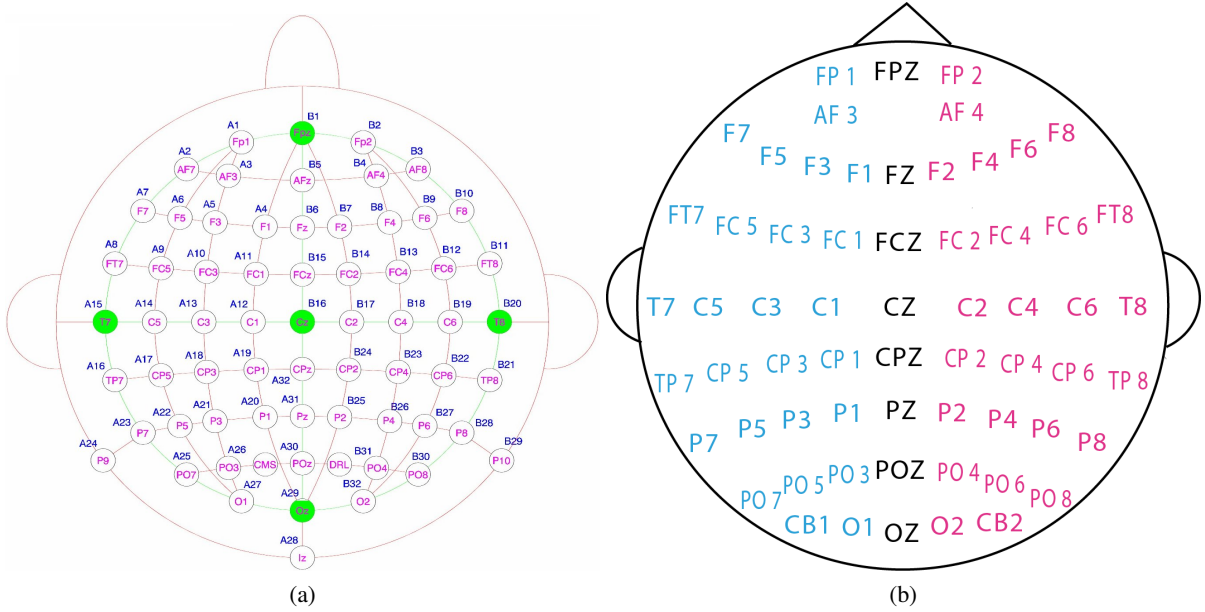


Figure 10. In this figure, (a) EEG-Video Action [59] Dataset EEG montage. We have selected the channels based on this arrangement for the studies involved EEG-Video Action dataset. (b) SEED [10, 64] Dataset EEG montage. We have selected the channels based on this arrangement for the studies involved SEED dataset.

```

11 'noseback_front': np.array([1, 2, 3, 4, 5, 6, 7,
12     8, 9, 10, 11, 12, 13, 14, 15, 16, 17, 18, 19,
13     20, 21, 22, 23], dtype=np.int32),
14 'noseback_back': np.array([33, 34, 35, 36, 37,
15     38, 39, 40, 41, 42, 43, 44, 45, 46, 47, 48,
16     49, 50, 51, 52, 53, 54, 55, 56, 57, 58, 59,
17     60, 61, 62], dtype=np.int32),
18 'lobes_frontal_left': np.array([1, 4, 6, 7, 8, 9,
19     16, 17, 18], dtype=np.int32),
20 'lobes_frontal_right': np.array([3, 5, 11, 12,
21     13, 14, 20, 21, 22], dtype=np.int32),
22 'lobes_parietal_left': np.array([34, 35, 36, 42,
23     43, 44, 45], dtype=np.int32),
24 'lobes_parietal_right': np.array([36, 39, 40, 47,
25     48, 49, 50], dtype=np.int32),
26 'lobes_occipital_left': np.array([51, 52, 53,
27     59], dtype=np.int32),
28 'lobes_occipital_right': np.array([55, 56, 57,
29     61], dtype=np.int32),
30 'lobes_temporal_left': np.array([15, 24, 33],
31     dtype=np.int32),
32 'lobes_temporal_right': np.array([23, 32, 41],
33     dtype=np.int32),
34 'lobes_frontal': np.array([1, 4, 6, 7, 8, 9, 16,
35     17, 18, 3, 5, 11, 12, 13, 14, 20, 21, 22, 2,
36     10, 19], dtype=np.int32),
37 'lobes_parietal': np.array([34, 35, 36, 42, 43,
38     44, 45, 36, 39, 40, 47, 48, 49, 50, 37, 46],
39     dtype=np.int32),
40 'lobes_occipital': np.array([51, 52, 53, 59, 55,
41     56, 57, 61, 54, 60], dtype=np.int32),
42 'lobes_temporal': np.array([15, 23, 24, 32, 33,
43     41], dtype=np.int32),

```

25 }

Listing 3. SEED dataset EEG cap locations

```

1 EEG_CAP_SHOT_V1 = {
2   'all': np.array([1, 2, 3, 4, 5, 6, 7, 8, 9, 10,
3     11, 12, 13, 14, 15, 16, 17, 18, 19, 20, 21,
4     22, 23, 24, 25, 26, 27, 28, 29, 30, 31, 32,
5     33, 34, 35, 36, 37, 38, 39, 40, 41, 42, 43,
6     44, 45, 46, 47, 48, 49, 50, 51, 52, 53, 54,
7     55, 56, 57, 58, 59, 60, 61, 62, 63, 64],
8     dtype=np.int32),
9   'noseback_left': np.array([1, 2, 3, 7, 6, 5, 4,
10     8, 9, 10, 11, 15, 14, 13, 12, 16, 17, 18, 19,
11     24, 23, 22, 21, 20, 25, 26, 27], dtype=np.
12     int32),
13   'noseback_center': np.array([33, 37, 38, 47, 48,
14     32, 31, 30, 29, 28], dtype=np.int32),
15   'noseback_right': np.array([34, 36, 35, 39, 40,
16     41, 42, 46, 45, 44, 43, 49, 50, 51, 52, 56,
17     55, 54, 53, 57, 58, 59, 60, 61, 63, 62, 64],
18     dtype=np.int32),
19   'noseback_Q1_right': np.array([34, 36, 35, 39,
20     40, 41, 42, 46, 45, 44, 43], dtype=np.int32),
21   'noseback_Q2_left': np.array([1, 2, 3, 7, 6, 5,
22     4, 8, 9, 10, 11], dtype=np.int32),
23   'noseback_Q3_left': np.array([16, 17, 18, 19, 24,
24     23, 22, 21, 20, 25, 26, 27], dtype=np.int32),
25   'noseback_Q4_right': np.array([56, 55, 54, 53,
26     57, 58, 59, 60, 61, 63, 62, 64], dtype=np.
27     int32),
28   'leftrightear_center': np.array([15, 14, 13, 12,
29     48, 49, 50, 51, 52], dtype=np.int32),
30   'noseback_front': np.array([1, 33, 34, 2, 3, 37,
31     36, 35, 7, 6, 5, 4, 38, 39, 40, 41, 42, 8, 9,
32     10, 11, 47, 46, 45, 44, 43], dtype=np.int32),
33   'noseback_back': np.array([16, 17, 18, 19, 32,
34     56, 55, 54, 53, 24, 23, 22, 21, 20, 31, 57,
35     58, 59, 60, 61, 25, 26, 30, 63, 62, 27, 29,
36     64, 28], dtype=np.int32),
37   'lobes_frontal_left': np.array([1, 2, 3, 4, 5, 6,
38     7, 9, 10, 11], dtype=np.int32),
39   'lobes_frontal_right': np.array([34, 35, 36, 39,
40     40, 41, 42, 46, 45, 44], dtype=np.int32),
41   'lobes_parietal_left': np.array([17, 18, 19, 24,
42     23, 22, 21, 20], dtype=np.int32),
43   'lobes_parietal_right': np.array([56, 55, 54, 57,
44     58, 59, 60, 61], dtype=np.int32),
45   'lobes_occipital_left': np.array([25, 26, 27],
46     dtype=np.int32),
47   'lobes_occipital_right': np.array([63, 62, 64],
48     dtype=np.int32),
49   'lobes_temporal_left': np.array([8, 15, 16],
50     dtype=np.int32),
51   'lobes_temporal_right': np.array([43, 52, 53],
52     dtype=np.int32),
53   'lobes_frontal': np.array([1, 2, 3, 4, 5, 6, 7,
54     9, 10, 11, 34, 35, 36, 39, 40, 41, 42, 46,
55     45, 44, 33, 37, 38, 47], dtype=np.int32),
56   'lobes_parietal': np.array([17, 18, 19, 24, 23,
57     22, 21, 20, 56, 55, 54, 57, 58, 59, 60, 61,
58     32, 31], dtype=np.int32),
59   'lobes_occipital': np.array([25, 26, 27, 63, 62,
60     64, 30, 29], dtype=np.int32),
61   'lobes_temporal': np.array([8, 15, 16, 43, 52,

```

53], dtype=np.int32),

25 }

Listing 4. EEG-Video Action dataset EEG cap locations

```

1 SEEDV_CAP = {
2   'all': np.array([1, 2, 3, 4, 5, 6, 7, 8, 9, 10,
3     11, 12, 13, 14, 15, 16, 17, 18, 19, 20, 21,
4     22, 23, 24, 25, 26, 27, 28, 29, 30, 31, 32,
5     33, 34, 35, 36, 37, 38, 39, 40, 41, 42, 43,
6     44, 45, 46, 47, 48, 49, 50, 51, 52, 53, 54,
7     55, 56, 57, 58, 59, 60, 61], dtype=np.int32),
8   'noseback_left': np.array([1, 4, 6, 7, 8, 9, 15,
9     16, 17, 18, 24, 25, 26, 27, 33, 34, 35, 36,
10     42, 43, 44, 45, 51, 52, 53, 58, 59], dtype=np.
11     int32),
12   'noseback_center': np.array([2, 10, 19, 28, 37,
13     46, 54, 60], dtype=np.int32),
14   'noseback_right': np.array([3, 5, 11, 12, 13, 14,
15     20, 21, 22, 23, 29, 30, 31, 32, 38, 39, 40,
16     41, 47, 48, 49, 50, 55, 56, 57, 61, 62],
17     dtype=np.int32),
18   'noseback_Q1_right': np.array([3, 5, 11, 12, 13,
19     14, 20, 21, 22, 23], dtype=np.int32),
20   'noseback_Q2_left': np.array([1, 3, 6, 7, 8, 9,
21     15, 16, 17, 18], dtype=np.int32),
22   'noseback_Q3_left': np.array([33, 34, 35, 36, 42,
23     43, 44, 45, 51, 52, 53, 56, 59], dtype=np.
24     int32),
25   'noseback_Q4_right': np.array([38, 39, 40, 41,
26     47, 48, 49, 50, 55, 56, 57, 61, 62], dtype=np.
27     int32),
28   'leftrightear_center': np.array([24, 25, 26, 27,
29     28, 29, 30, 31, 32], dtype=np.int32),
30   'noseback_front': np.array([1, 2, 3, 4, 5, 6, 7,
31     8, 9, 10, 11, 12, 13, 14, 15, 16, 17, 18, 19,
32     20, 21, 22, 23], dtype=np.int32),
33   'noseback_back': np.array([33, 34, 35, 36, 37,
34     38, 39, 40, 41, 42, 43, 44, 45, 46, 47, 48,
35     49, 50, 51, 52, 53, 54, 55, 56, 57, 58, 59,
36     60, 61, 62], dtype=np.int32),
37   'lobes_frontal_left': np.array([1, 4, 6, 7, 8, 9,
38     16, 17, 18], dtype=np.int32),
39   'lobes_frontal_right': np.array([3, 5, 11, 12,
40     13, 14, 20, 21, 22], dtype=np.int32),
41   'lobes_parietal_left': np.array([34, 35, 36, 42,
42     43, 44, 45], dtype=np.int32),
43   'lobes_parietal_right': np.array([38, 39, 40, 47,
44     48, 49, 50], dtype=np.int32),
45   'lobes_occipital_left': np.array([51, 52, 53,
46     54], dtype=np.int32),
47   'lobes_occipital_right': np.array([55, 56, 57,
48     61], dtype=np.int32),
49   'lobes_temporal_left': np.array([15, 29, 33],
50     dtype=np.int32),
51   'lobes_temporal_right': np.array([23, 32, 41],
52     dtype=np.int32),
53   'lobes_frontal': np.array([1, 2, 3, 4, 5, 6, 7,
54     8, 9, 10, 11, 12, 13, 14, 16, 17, 18, 19, 20,
55     21, 22], dtype=np.int32),
56   'lobes_parietal': np.array([34, 35, 36, 37, 38,
57     39, 40, 42, 43, 44, 45, 46, 47, 48, 49, 50],
58     dtype=np.int32),
59   'lobes_occipital': np.array([51, 52, 53, 54, 55,
60     56, 57, 59, 60, 61], dtype=np.int32),
61   'lobes_temporal': np.array([15, 29, 33, 23, 32,

```



Figure 11. Additional Results on the SEED [10, 64] dataset. Each row is a different frame condition and is generated using EEG visual features.

```
41], dtype=np.int32),}
```

Listing 5. SEED-DV dataset EEG cap locations

## E. Additional Qualitative Results

Figure [11, 12, 13] shows additional results on the SEED [10, 64], EEG-Video Action [59] and SEED-DV [28] datasets.

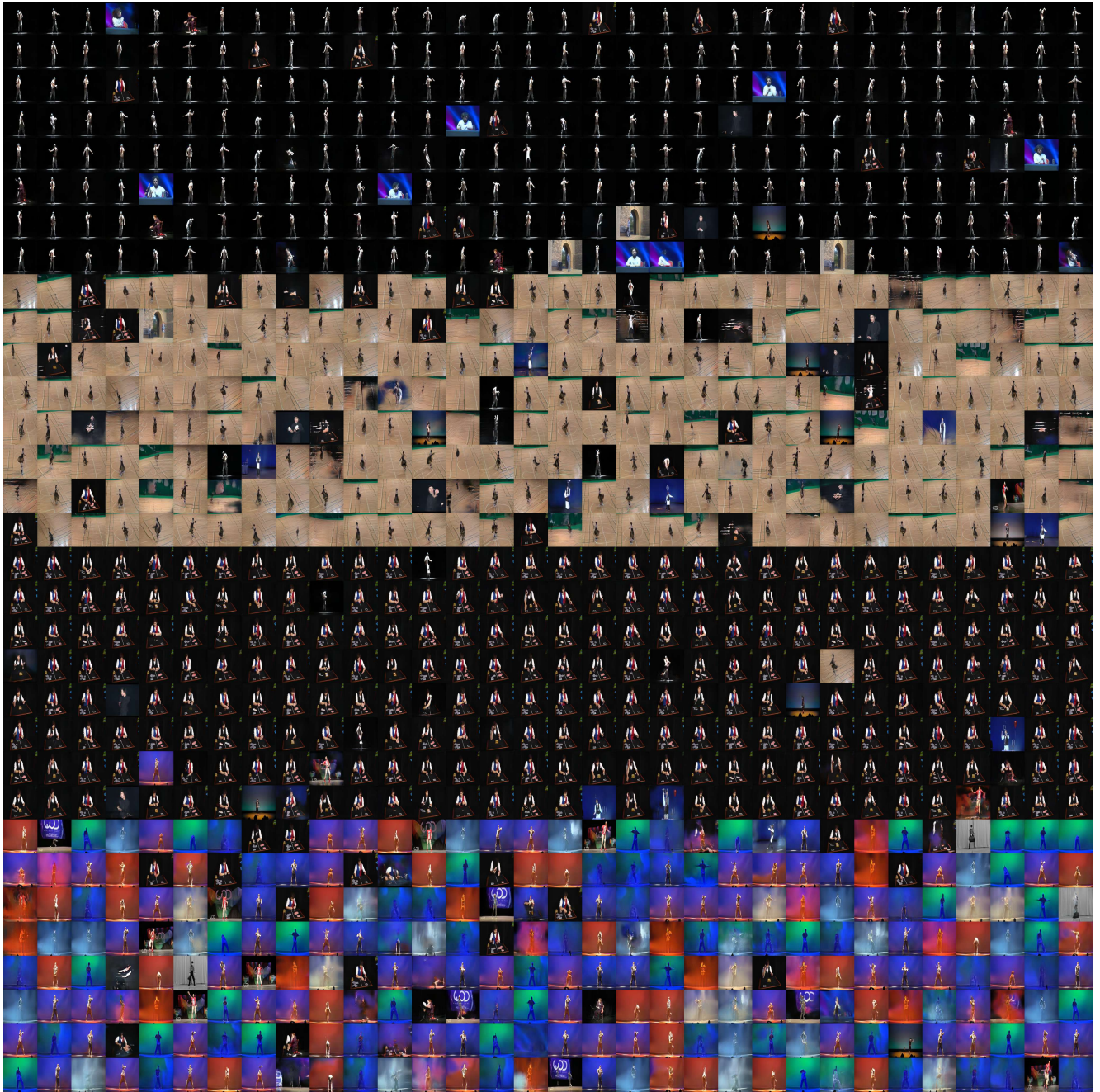


Figure 12. Additional Results on the EEG-Video Action [59] dataset. Each row is a different frame condition and is generated using EEG visual features.



Figure 13. Additional Results on the SEED-DV [28] dataset. Each row is a different frame condition and is generated using EEG visual features.